11,08,10

The influence of H-H interaction and alternating electric field on hydrogen desorption processes from partially hydrogenated graphene

© A.I. Podlivaev

National Research Nuclear University „MEPhI“,
Moscow, Russia

E-mail: AIPodlivayev@mephi.ru

Received September 2, 2025
Revised September 22, 2025
Accepted October 24, 2025

Multiscale modeling of graphene hydrogenation under the action of an alternating electric field was carried out. Microscopic parameters describing hydrogen desorption were calculated based on molecular dynamics within the framework of the non-orthogonal tight-binding model. These parameters were used in the chemical kinetics equation, which allows describing the dynamic behavior of hydrogen concentration over macroscopic times. The possibility of controllably forming inhomogeneities in the hydrogen distribution on the graphene surface under the action of an external electric field was shown. Under conditions typical for graphene hydrogenation experiments (temperature 350 K, hydrogen saturation time 2 hours), the optimal frequency of the external electric field was $516 \cdot 10^{12}$ rad/s with an electric field amplitude in the range of 1−0.01 V/nm. The resonant action of such a field makes it possible to create regions on the graphene surface in which the hydrogen concentration is 3−0.02 % of the maximum achieved in the absence of an electric field.

Keywords: Hydrogenation of graphene, graphane, desorption, activation energy, molecular dynamics.

DOI: 10.61011/PSS.2025.10.62644.239-25

1. Introduction

Synthesis of graphene [1] — planar structure (graphite monolayer) with high strength [2] and mobility of charge carriers [3] — have stimulated the extensive research of planar carbon structures combined with individual elements, molecules, and various types of substrate.

The impact of external effects on graphene properties is currently extensively investigated because it can be applicable for creation of graphene electronic components such as transistors, microcapacitors, biosensors, etc. (see,for example, [4–8]). In paper [9] graphane was predicted in theory and further synthesized [10] — a monolayer of graphene, fully saturated with oxygen from both sides. The high hydrogen content in graphane does not exclude its use in hydrogen energy, and the combination of conductive graphene and dielectric graphane does not exclude applications in graphene electronics. The feasibility of such a combination depends on the thermal stability of fully or partially hydrogenated graphene. Many experimental and theoretical papers have been devoted to studying the characteristics of graphene with varying degrees of hydrogenation with variable concentrations of chemisorbed hydrogen (e. g. see, [10–21]).

In addition to the thermal stability of hydrogen clusters on the graphene surface, for the practical implementation of graphene electronics based on graphene-graphane composition, the technology of applying a hydrogen pattern to the graphene plane is necessary. A possible factor that makes it possible to locally influence the process of hydrogen desorption is the effect on hydrogenated graphene of an external electric field (EEF) perpendicular to the graphene surface. The effect of EEF (perpendicular to the graphene plane) on the hydrogen-graphene system was studied in [22]. In this study, it was shown that an external permanent EEP with a voltage of ~ 1 V/Å of the corresponding sign may significantly intensify the process of graphene hydrogenation with atomic hydrogen. In [16], the effect of an external variable force applied to one graphane atom — fully hydrogenated graphene was investigated. In this work, it was shown that in the case of resonance of an external force and one of the phonon modes of graphane, it is possible to enhance the process of dehydrogenation of this structure. Previously, the desorption of gases from the metal surface under acoustic influence was studied in [17], and the desorption of halogen and alkali metal atoms from the graphene surface — in [18]. In the study [19], the intensification of the annealing process of radiation defects in silicon carbide is hypothetically explained by the resonant effect of acoustic phonons of the appropriate frequency.

The method of forming such structures is theoretically investigated in [23]. In this study, general interatomic interaction of C-H system is defined within the Nonorthogonal Tight-Binding Model — NTBM, [24]) with dispersion corrections [25]. The main interaction in NTBM is defined as the sum of the energies of the valence electrons system and the pair interaction of atomic nuclei with the remaining (non-valence) electrons. The dispersion corrections [25] are paired, long-range, and small compared to basic potential [24]. The electronic energy of C-H system is determined by solving the Schrodinger equation with the Hamiltonian

in the strong coupling approximation. As a result, the general interatomic interaction incorporates many bodies. In [23], the possibility of inhomogeneous hydrogenation of the graphene surface due to the local action of EEF on the hydrogenated sample was investigated. In this case, the frequency of EEF coincides with the resonant frequency of vibrations of hydrogen atoms covalently bound to the graphene core. In this study, it was shown that this effect intensifies the process of hydrogen desorption, which allows the controlled creation of hydrogen-depleted regions. Also in [23], it was shown that the surface diffusion of chemisorbed hydrogen from a saturated to a hydrogen-depleted region does not significantly blur the boundary between these regions. However, in [23] only the case of low concentrations of chemisorbed hydrogen was considered. Because of this, H-H interaction on the graphene surface was neglected. The H-H interaction in a C-H cluster with a many-body potential conditionally means the indirect interaction of hydrogen atoms caused by a change in the electronic structure of the system when hydrogen atoms are shifted against a backdrop of a slight change in the coordinates of the carbon core atoms.

In this paper, the possibility of forming two regions with different levels of hydrogenation through the local action of an external alternating electric field is studied. Such hydro-treating modes are selected where the concentration of hydrogen in the region impacted by EEF will be low (hereinafter — depleted in hydrogen), and in the region adjacent to it (without exposure) the concentration of hydrogen Q is comparable to the maximum possible ($Q \sim 1$, and further, this region is designated as a hydrogen-enriched region).

In this paper, a combination of two approaches is used to calculate the concentration of chemisorbed hydrogen in depleted and enriched regions. In the first approach, within the nonorthogonal tight-binding model (NTBM) [24]) with dispersion corrections [25], we used the method of molecular dynamics to find the activation energies and appropriate frequency factors of hydrogen desorption from the surface of hydrogenated graphene. In the following approach, based on the activation energies and the corresponding frequency factors obtained in the present study and in [23], hydrogen concentrations are determined in two regions, one of which is under the influence of EEF, and the other is not affected.

2. Description of model and calculation method within NTBM

The calculation method based on NTBM [24,25] has lower precision compared to *ab initio* methods but requires less computational power. A software implementation of the non-orthogonal strong coupling model in FORTRAN is published in [26]. The potential based on tight-binding approximation has been successfully applied in modeling of carbon clusters, and clusters containing hydrogen, nitrogen, and oxygen atoms in addition to carbon atoms (see, for example, papers [13,23–30] and references in them).

Similar to [23] for the study of graphene the supercell 2×2 of $C_{64}H_N$ was used where $N = 1$, 32 and 64 — number of hydrogen atoms in the supercell. The Cartesian coordinates of the cell atoms are oriented so that the axis Z is perpendicular to the graphene base (the plane least deviating from the carbon atoms). In this paper, periodic conditions are assumed with three vectors forming a periodicity cell. The Cartesian coordinates of these vectors are equal $(13.309, 0; 0)$, $(1.901, 13.173, 0)$, $(0, 0, \infty)$ (Å). Just as in [23], only the force component normal to the graphene surface F_z was considered. In the framework of the simplest quasi-stationary approximation in [23] the magnitude of this force per atom of a cluster with index i was assumed to be as follows: $F_z = q_i E_Z \sin(\omega t)$, where t — time, ω — EEF frequency, q_i — the Millikan charge of the corresponding atom. The Schrodinger equation, which makes it possible to describe the cluster's electronic system within NTBM, does not take into account the impact of the EEF. It should be stressed that when this paper (similar as in [23]) describes frequency ω, then cyclic (angular or circular) frequency is implied in units rad/s.

In the absence of EEF the modeling was carried out within the framework of microcanonical assembly [31]. In this paper, we study the possibility of creating a low concentration of hydrogen in a region irradiated by an external electric field, while outside this region its concentration is comparable to the maximum possible. In case of zero EEF for the hydrogen concentration $Q = 0$ the activation energy and desorption frequency factor are identical to those outlined in [23] for the cluster $C_{64}H_1$. Just as in one of the variants considered in [23], the value of the strength of the normal component of the electric field $E_Z = 0.1$ V/Å is chosen. This value was chosen as extremely low, which makes it possible to simulate the desorption process with a reasonable consumption of computer resources. At lower values of E_Z, the statistical error in determining the average desorption time does not allow us to confidently distinguish this value from that obtained at $E_Z = 0$. The resonance frequency of this field ω_{res} which has the greatest effect on graphene dehydration at $E_Z = 0.1$ V/Å and $Q \ll 1$ is equal $516 \cdot 10^{12}$ rad/s [23].

Within the NTBM approximation, the desorption time of a hydrogen atom τ_{desorb} was determined using the molecular dynamics (MD) method for various temperatures. As the temperature decreases, the probability of the desorption process decreases significantly, which increases the time for computer calculations of the evolution of the system from the initial state to the moment of separation of the hydrogen atom from graphene. When calculating on modern PCs, modeling of these processes within the framework of the accepted model is possible in the range of relatively high temperatures (from 1300 K and higher depending on the initial concentration of chemisorbed hydrogen). However, the region of lower temperatures (below 1000K) is of practical interest for graphene hydrogenation processes.

Therefore, it is necessary to extrapolate the temperature dependence of τ_{desorb} to the low temperature range. In the absence of EEF, the determination of the value τ_{desorb} can be carried out by extrapolation based on the Arrhenius formula

$$\frac{1}{\tau_{\text{desorb}}} = A \exp\left(\frac{-E}{k_B T}\right), \tag{1}$$

where T — temperature, and E and A — activation energy and frequency factor of desorption, k_B — Boltzmann constant.

Approximate expression (1) is obtained to describe thermalized systems, and in the case of a nonzero EEF, there is an additional nonequilibrium external effect (energy exchange of a field with phonon modes of the $C_{64}H_{32}$ structure, in which there is a significant change in the length of the C-H bond). However, as an extrapolating function to the low temperature region, the expression (1) looks preferable to other types of extrapolation (power-law, exponential, etc.).

The standard procedure for determining activation energies and frequency factors was carried out using the MD method as follows. The atoms of the cluster $C_{64}H_{32}$ were given initial velocities, which were determined by the Maxwell distribution corresponding to the initial temperatures $T = 1300$, 1350, 1400, dots, 1800, 1850 K (a total of 28 different temperatures). The atoms were also given initial displacements corresponding to the initial temperature. The amplitudes of the initial stochastic displacements were selected so that the increase in the potential energy of the cluster (due to temperature) was equal to the total kinetic energy of the atoms. The numerical solution of the problems of molecular dynamics was carried out using Verlet algorithm with a time step of 0.3 fs. The logarithm of the desorption time of one of the hydrogen atoms versus reciprocal temperature makes it possible to determine the activation energies and frequency factors of the corresponding processes within the framework of regression analysis.

The values E and A in cluster $C_{64}H_N$ with the hydrogen atoms number $N = 32$ are found in this study by MD method. The data for $N = 1$ and 64 corresponded to those given in papers [23] and [32]. In the general case, the dependence of the values E and A on the concentration of adsorbed atoms is not linear (e.g., see [33–36]). Detailed determination of these characteristics at values N other than 1, 32 and 64 requires excessive computational power and, therefore, was carried out by simplified linear interpolation from data obtained at $N = 1$, 32 and 64. Maximal possible amount of N in the cluster of graphane $C_{64}H_N$ is equal 64. Further, it is considered that relative hydrogen concentrations $Q = 1$, 0.5 and 0 for $N = 64$, 32 and 1, respectively. Such a conditional correspondence between the values Q and N implies that the cluster containing 64 carbon atoms is large enough, and its increase will not lead to a noticeable change in the desorption characteristics of a single hydrogen atom located on the graphene surface. The linear interpolation of the activation energy $E(Q)$, which depends on the average concentration of hydrogen atoms Q, is represented as follows:

$$E(Q) = \begin{cases} E(Q=0) + 2Q \cdot \big(E(Q=0.5) - E(Q=0)\big); \\ 0 \le Q \le 0.5 \\ 2\big[E(Q=1) \cdot (Q-0.5) + E(Q=0.5) \cdot (1-Q)\big]; \\ 0.5 \le Q \le 1 \end{cases}. \tag{2}$$

Linear interpolation of the frequency desorption factor $A(Q)$ is performed in a similar way.

To study the evolution of a system through the equations of chemical kinetics, configurations that can be adequately described within the framework of approximations with a locally uniform distribution of hydrogen atoms are of interest. If the configurations of clusters $C_{64}H_{64}$ and $C_{64}H_1$ with uniform distribution of hydrogen are defined in the only way (with accuracy to the translational displacement of the hydrogen system), then, in the cluster $C_{64}H_{32}$ the hydrogen atoms may be arranged in different ways. In this paper, three ways of arranging hydrogen on a graphene core were considered. For all methods, the dimensions of the periodic cell corresponded to the dimensions of the optimal graphene cell, which lacks hydrogen (the cell dimensions are indicated above). In each variant, the coordinates of all atoms were relaxed. The equilibrium configuration was determined by the gradient relaxation method. The maximum value of interatomic forces in equilibrium structures $C_{64}H_{32}$ in this case did not exceed the value $\sim 10^{-8}$ eV/Å. The shapes of the first two clusters are given in Figures 1, *a* and 1, *b*. In the third case, 32 hydrogen atoms were located stochastically above and below the carbon atoms, but any carbon atom covalently bonded to no more than one hydrogen atom. 32 variants of the stochastic distribution of hydrogen were considered (half of the hydrogen atoms were removed from the cluster $C_{64}H_{64}$ using a random sample). This allowed us to determine the average cluster's potential energy and the standard statistical error of determining this value. Calculations have shown that the cluster has the minimum potential energy, the top view of which is shown in Figure 1, *a*. In this cluster, the hydrogen atoms are arranged in chains. In this case, the hydrogen chains located above the carbon base are parallel to the chains located below the carbon base. An alternative to this structure is the cluster shown in Figure 1, *b*. In this cluster the „upper" hydrogen chains are perpendicular to the „lower" ones. Deviations of the optimal cluster's potential energy from the potential energy of the cluster shown in Figure 1, *b* is equal to 0.10 eV/(hydrogen atom). The potential energy averaged over 32 variants of clusters with a random distribution of hydrogen differs from the optimal energy by 0.19 ± 0.01 eV/(hydrogen atom). For further modeling, the cluster shown in Figure 1, *a*, is selected as the most stable one. Figure 1, *c* provides the 3D image of this cluster. A slight difference in the energies of these three types of different arrangements of hydrogen (the two shown

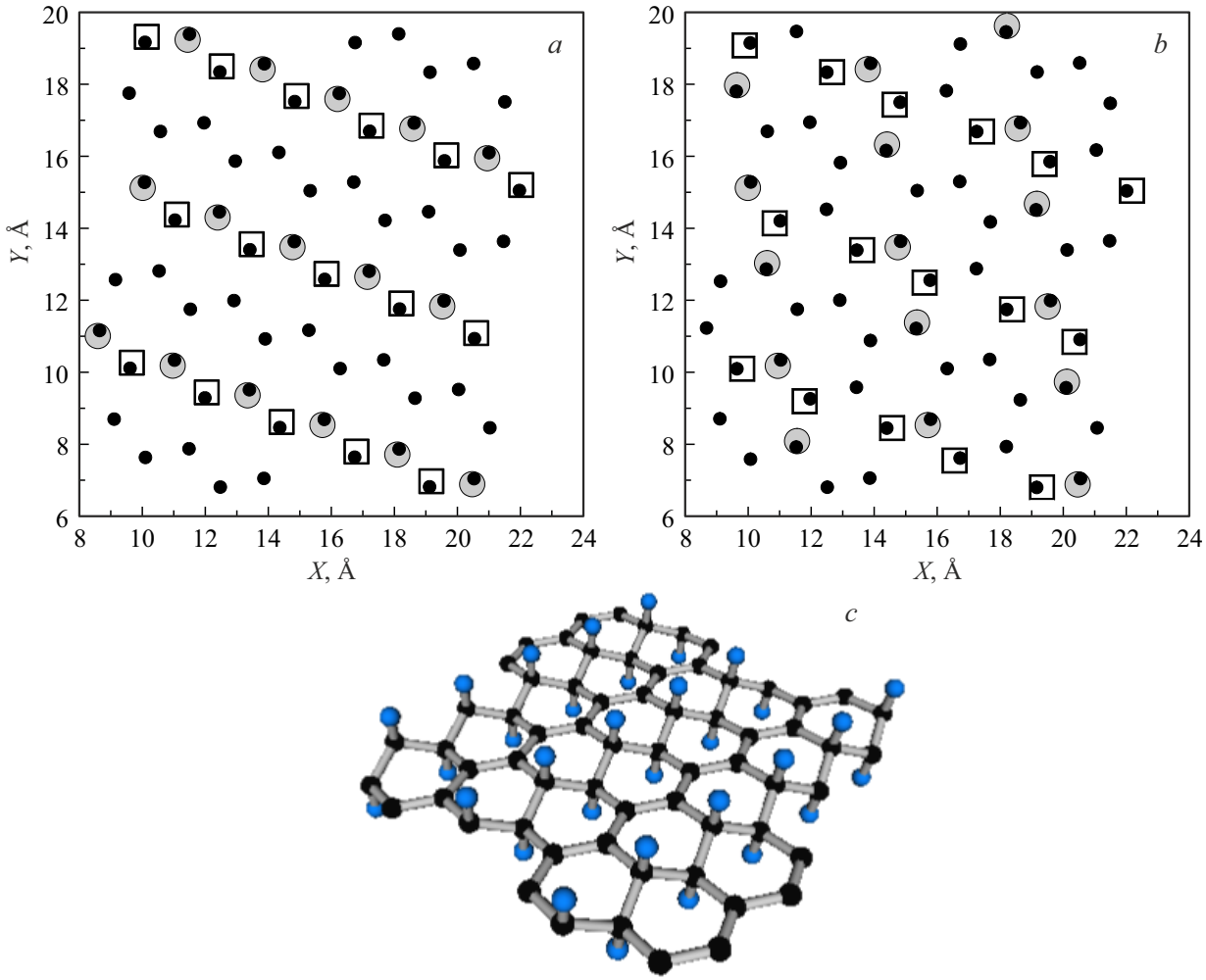

Figure 1. Various types of the calculated cell with clusters $C_{64}H_{32}$. (*a*) — form of the most stable calculated cluster (plan view). (*b*) — an alternative form of the calculated cluster in which the hydrogen chains located above the graphene base are perpendicular to the chains located below the base (plan view). Large gray circles — hydrogen atoms located under carbon atoms, colorless squares — hydrogen atoms located above carbon atoms. (*c*) — three-dimensional image of the most stable cluster. Large blue circles — hydrogen atoms, black circles — carbon atoms.

in Figure 1 and stochastic) allows us to hope that in these configurations such desorption characteristics as desorption activation energies will not differ significantly. Indeed, the desorption energies of a hydrogen atom upon its separation from graphene and graphane are equal, respectively, to 1.14 [23] and 2.26 [32] eV, which significantly exceeds 0.19 eV/(hydrogen atom) of deviations of potential energies in clusters $C_{64}H_{32}$ of various types.

3. Calculation method. The equation of chemical kinetics

The equation of chemical kinetics, found from the mean field approximation, allows us to qualitatively describe the temporal evolution of the studied structure over a wide temperature range. The detectable value in this approach is the local average concentration of Q hydrogen atoms above and below the carbon core (see Figure 1, *a*).

The equation of chemical kinetics (the equation of the balance of the density of hydrogen atom fluxes) can be represented as follows:

$$dQ(t)/dt = \Phi(Q(t)),$$

$$\Phi(Q) = (1-Q)/\tau_{\text{adsorb}} - Q/\tau_{\text{desorb}}(Q), \qquad (3)$$

where t — time, τ_{adsorb} — typical adsorption time of atomic hydrogen onto pure (non-hydrogenated) graphene. The first term in the right-hand side of the second line of the equation (3) describes an increase in hydrogen concentration due to the chemisorption of atomic hydrogen from the environment. The intensity of adsorption is determined by the characteristic time τ_{adsorb} of saturation of the primary graphene surface with hydrogen atoms and proportional to the concentration of hydrogen vacancies $(1-Q)$. The

last term of the right side of the equation (3) describes the process of chemical desorption with characteristic time τ_{desorb}, which complies with Arrhenius law (1) (while activation energy and frequency factor being dependent on Q). The equation (3) is added with the following initial conditions:

$$Q(t=0)=0. \tag{4}$$

This condition implies that from the initial moment the primarily pure graphene becomes saturated under the influence of an external alternating electric field.

The value $1/\tau_{\text{adsorb}}$ is limited from above by the frequency of collisions of hydrogen atoms with the graphene surface, since not every collision of a hydrogen atom with the pure graphene surface is accompanied by the formation of a covalent C-H bond. Considering atomic hydrogen as an ideal gas, this limitation will be expressed as follows: $1/\tau_{\text{adsorb}} < n \cdot \bar{\upsilon} \cdot S/4$. In this expression the variables $n\,(\text{at/m}^3)$, $\bar{\upsilon}\,(\text{m/s})$ and $S\,(\text{m}^2/\text{at})$ denote, respectively, the atomic density of hydrogen in the environment, the average velocity of a hydrogen atom, and the surface area of graphene per one carbon atom. Under normal conditions (the partial pressure of atomic hydrogen is $\sim 10^5$ Pa, temperature $T \sim 300$ K), this limitation takes the following form: $1/\tau_{\text{adsorb}} < 0.5 \cdot 10^9\,(1/\text{s})$. At atmospheric pressure and temperature $T \sim 1000$ K the limitation is expressed as follows: $1/\tau_{\text{adsorb}} < 0.27 \cdot 10^9\,(1/\text{s})$. In paper [10], the characteristics of a gas mixture from which graphene is saturated with atomic hydrogen are given. The partial pressure of hydrogen in the argon-hydrogen mixture was ~ 10 Pa. At the same time, a significant part of the hydrogen was in an inert molecular state. The time of complete saturation of graphene with hydrogen, given in [10], was about two hours.

The frequency desorption factor $A(Q=0.5)$, which determines the frequency of separation of at least one of 32 hydrogen atoms from the cluster $C_{64}H_{32}$ is 32 times greater than the frequency factor of separation of one atom with a fixed number (the frequency factor of separation of a hydrogen atom with number 1 in 32 is less than the separation factor in case when any of the 32 atoms can come off). A similar remark also applies to the redefinition of the frequency factor $A(Q=1)$, obtained from [32]. The activation energies and their corresponding frequency factors, obtained taking into account the listed corrections, are presented in the next section.

4. Results

Within NTBM the desorption characteristics of cluster $C_{64}H_N$ are provided and given in the Table 1.

The frequency factors and activation energies in lines of Table 1 marked by «*» were obtained by method of linear interpolation between the two marks $E_Z = 0$ and 0.1 eV/Å.

Given the spread of data in Table 1 for $Q=1$ the value τ_{desorb} lies in the interval $10^{-4} < \tau_{\text{desorb}} < 8 \cdot 10^{-3}$ s at $T = 1000$ K, and in the interval $10 < \tau_{\text{desorb}} < 4 \cdot 10^3$ s at $T = 700$ K. These data do not contradict the results of the experimental work [10]. In this work, the complete release of hydrogen from graphane was observed as a result of graphane annealing during the day at a temperature of 700 K. It should be emphasized that in the process of saturation of graphene with atomic hydrogen, the value of τ_{desorb} changes by several orders of magnitude from the initial concentration $Q=0$ to the limiting concentration $(Q=1)$ at a temperature of 700 K. Given this temperature and concentration $Q=0$ $(N=1)$ in the absence of EEF and under the impact of EEF the values τ_{desorb} are equal $8 \cdot 10^{-7}$ and $2 \cdot 10^{-7}$ s, respectively.

Table 1. Energies of activation E and corresponding frequency desorption factors A of cluster $C_{64}H_N$

$N(Q)$, [literature]	E_Z, eV/Å	E, eV	A, 1/s
1(0), [23]	0	1.14 ± 0.19	$(1.99 \pm 0.31) \cdot 10^{14}$
	0.1	0.96 ± 0.20	$(5.1 \pm 0.8) \cdot 10^{13}$
	0.01*	1.12	$1.18 \cdot 10^{14}$
	0.001*	1.138	$1.975 \cdot 10^{14}$
32(0.5)	0	1.62 ± 0.14	$(7.7 \pm 1.5) \cdot 10^{13}$
64(1), [32]	0	2.46 ± 0.17	$(2.9 \pm 0.7) \cdot 10^{15}$

Calculations have shown that alternating EEF with frequency $\omega_{\text{res}} = 516 \cdot 10^{12}$ rad/s has a noticeable effect only on the characteristics of the cluster $C_{64}H_1$. Deviation from this resonant frequency significantly reduces the strength of EEF effect on this system. In [23] it was demonstrated that variation of frequency from the optimal ω_{res} (destroying the cluster $C_{64}H_1$ by resonance) to $526 \cdot 10^{12}$ rad/s results in decline of the field-induced oscillations amplitude by 1.9 times. In cluster $C_{64}H_{32}$ two maximal phonon frequencies are equal $570 \cdot 10^{12}$ rad/s and $290 \cdot 10^{12}$ rad/s. In the cluster $C_{64}H_{64}$ two maximal phonon frequencies are equal $590 \cdot 10^{12}$ rad/s and $250 \cdot 10^{12}$ rad/s. Thus, the resonant frequency falls into the band gap of clusters $C_{64}H_{32}$ and $C_{64}H_{64}$ and does not significantly affect the phonon system. A similar effect of the decline in EEF influence on graphane during hydrogen desorption from it was noted earlier in the theoretical study [16]. In cluster $C_{64}H_1$ there's a single mode with a frequency of $526 \cdot 10^{12}$ rad/s. The frequency of the subsequent mode is equal $294 \cdot 10^{12}$ rad/s. This feature of the phonon spectrum also justifies taking into account the influence of only electric field component E_Z on the cluster oscillation. The only phonon mode that resonates with EEF is the high-frequency mode in which the hydrogen atom is shifted in the direction of the axis Z. The frequencies of the remaining modes, which may be shifted in the directions of the axes X and Y, have frequencies noticeably lower than the maximum. Therefore, in this study, the components of E_X and E_Y fields are neglected

due to the lack of resonant interaction between them and the phonon system of the cluster.

Figure 2 shows the dependence of the time derivative $\Phi(Q)$ at different temperatures, as well as the parameters τ_{adsorb} and E_Z. The break in the graphs in Figure 2, *a* is caused by a break in the piecewise linear interpolation of $\tau_{\text{adsorb}}(Q)$ (1, 2) dependence in point $Q = 0.5$. In Figure 2, *b* and 2, *c* for $Q = 0.5$, the second term in the right-hand side of equation (3) is small, so there is no break in the curves in these figures.

Figure 2 shows that with large values τ_{adsorb} the equation (3) has 3 stationary points ($\Phi(Q) = 0$). The concentration values at these points are hereinafter referred to as $Q_{\min}$, Q_{mid} and $Q_{\max}$ in accordance with their magnitudes. In all lines in Figure 2 the magnitude of $Q_{\max}$ is practically equal to unit. For small values of τ_{adsorb}, a single stationary point with magnitude $Q_{\max}$ is observed. The transition from the mode with three stationary points to the mode with one occurs at the boundary value of the adsorption time, which is further denoted as τ^c_{adsorb}. At $\tau_{\text{adsorb}} = \tau^c_{\text{adsorb}}$ the concentrations $Q_{\min} = Q_{\text{mid}}$, and concentration in this point is further denoted as Q^C. The values of τ^c_{adsorb} and Q^C at different values of temperature and amplitude of EEF are given in Table 2.

At concentration $Q = Q_{\text{mid}}$ the derivative with respect to the right-hand side of equation (3) $d\Phi(Q_{\text{mid}})/dQ_{\text{mid}} > 0$. As a result, a stationary point with a given concentration is unstable. The small deviation of the concentration from the value Q_{mid} increases with time. In contrast, stationary points with concentrations $Q = Q_{\min}$ or $Q = Q_{\max}$ are stable. The small deviation of the concentration from these values declines exponentially over time. Because of the existence of two stable points and one intermediate unstable stationary point $Q = Q_{\text{mid}}$, the initial condition (4) becomes essential. This condition determines not only the dynamics of the equilibrium concentration $Q(t = +\infty)$, but also the value of this concentration. Indeed, if the effect of EEF does not begin simultaneously with the hydrogenation process, but at the moment when the concentration exceeds the value $Q_{\text{mid}}(Q(t = 0) > Q_{\text{mid}})$, the function $\Phi(Q)$ falls into the right-hand region of positive values (see Figure 2). As a result, the concentration of adsorbed hydrogen under the influence of EEF rises and tends to the value of $Q_{\max}$, and not to the desired value of $Q_{\min}$.

Let's decompose the function $\Phi(Q)$ at a stable stationary point $Q = Q_0(Q_0 = Q_{\min}, Q_{\max})$ in the Taylor series up to the linear term, taking into account the concentration dependence of the values $E(Q)$ and $A(Q)$. Substituting this expansion into the equation (3) taking into account Arrhenius law (1) gives the following linear differential equation:

$$dQ(t)/dt = (Q_0 - Q)/\tau_0,$$

$$1/\tau_0 = 1/\tau_{\text{adsorb}} + \left(1 + Q_0 \frac{dA(Q_0)}{dQ_0}/A(Q_0) - Q_0 \frac{dE(Q_0)}{dQ_0}/(k_B T)\right)/\tau_{\text{decorb}}(Q_0), \quad (5)$$

with the initial condition (4). The value τ_0 in equation (5) characterizes the time of local relaxation of concentration Q to the stationary concentration Q_0. Note that for the value $\tau_{\text{desorb}}(Q_{\max})$ obtained from the interpolation formula (2) and the Arrhenius law (1) for all sets of parameters $\{\tau_{\text{adsorb}}, E_Z, T\}$ (which are shown in Figure 2 and in the Table 2) a strong inequality was true. $1/\tau_{\text{adsorb}} \gg 1/\tau_{\text{desorb}}(Q_{\max})$. As a consequence, from the equation (5) the values τ_{adsorb} and $\tau_0(Q_{\max})$ are almost identical.

When graphene is formed inhomogeneously saturated with hydrogen, it is assumed that the initially purified graphene is placed in a hydrogen medium with a preset value of τ_{adsorb} at a temperature of T. At the same time, a part of the graphene surface is exposed to EEF. As a result of hydrogen saturation of both regions, the concentration in the irradiated part should reach the value of $Q_{\min}$, and in the shaded area- the value of $Q_{\max}$. During the evolution defined by equation (3) the concentration Q from zero rises to the concentration of the nearest stationary point ($Q_{\min}$ at $\tau_{\text{adsorb}} > \tau^c_{\text{adsorb}}$ or $Q_{\max}$ $\tau_{\text{adsorb}} < \tau^c_{\text{adsorb}}$). The fulfillment of these two inequalities provides the following condition for the formation of an inhomogeneous concentration of hydrogen chemisorbed on the graphene surface:

$$\tau^c_{\text{adsorb}}(E_Z = 0) < \tau_{\text{adsorb}} < \tau^c_{\text{adsorb}}(E_Z = 0.1\,\text{eV/Å}) \quad (6)$$

For the temperature $T = 350\,\text{K}$ the inequality (6) is expressed as follows $149 < \tau_{\text{adsorb}} < 11400\,\text{s}$. For saturation during $\tau_{\text{adsorb}} = 2$ hours the values $Q_{\min}(E_Z = 0.1\,\text{eV/Å})$ and $Q_{\max}(E_Z = 0)$ are equal, respectively to 0.0002 and 1. The characteristic times for setting the equilibrium concentrations τ_0 in the regions irradiated by external field and non-irradiated regions are 1.4 and 7200 s, respectively.

The equation of chemical kinetics (3) with complementary expressions (1), (2) and (4) make it possible to determine the dynamics of hydrogen accumulation at any values of the amplitude E_Z if the activation energy and the frequency desorption factor are known for this field strength value. At $E_Z \ll 0.1\,\text{eV/Å}$ calculation of desorption characteristics by method of molecular dynamics requires excessive computational power. In [23], for small values of E_Z, the activation energy and frequency desorption factor were determined by linear interpolation between two interpolation nodes $E_Z = 0$ and 0.1 eV/Å. The results of equivalent interpolation for $E_Z = 0.01$ and 0.001 eV/Å are illustrated in Table 1 (denoted by symbol «*»). For temperature $T = 350\,\text{K}$, the limits of intervals of τ_{adsorb} are defined (see expression (6)) at which it is possible to form an inhomogeneous distribution of chemisorbed hydrogen).

For $E_Z = 0.01\,\text{eV/Å}$ the expression (6) will be written as follows: $10150 < \tau_{\text{adsorb}} < 11400\,\text{s}$. For $\tau_{\text{adsorb}} = 10150\,\text{s}$ the time during which the concentration in the shadow region reaches 0.99 is equal 49907 s.

For $E_Z = 0.001$ the expression (6) will be written as follows: $10850 < \tau_{\text{adsorb}} < 11400\,\text{s}$. For $\tau_{\text{adsorb}} = 10850\,\text{s}$ the time during which the concentration in the shadow region reaches 0.99 is 52137 s.

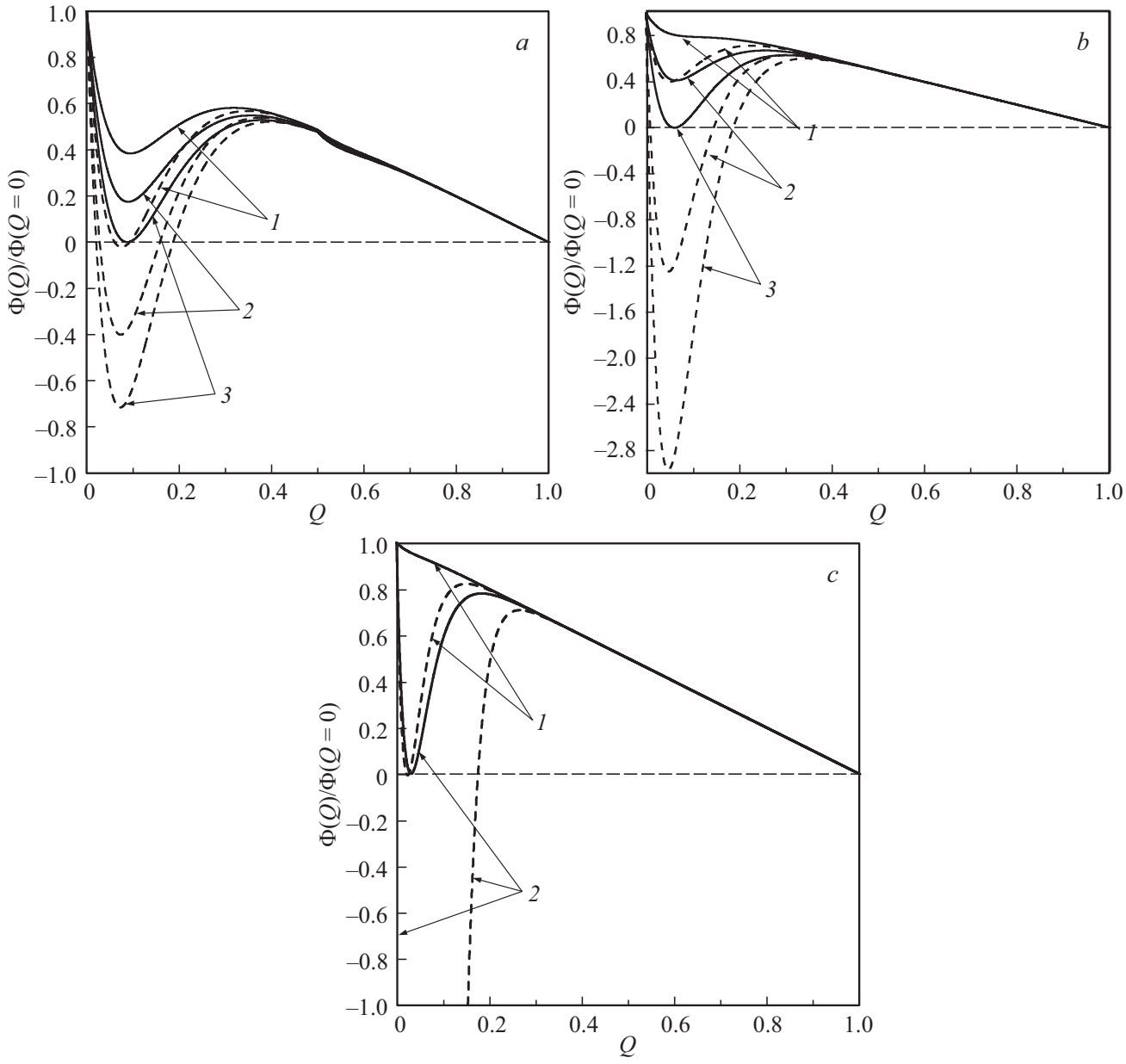

Figure 2. Dependence $\Phi(Q)/\Phi(Q=0)$. Solid lines correspond to the dependence $\Phi(Q)/\Phi(Q=0)$ in the absence of EEF ($E_Z = 0$). The dashed lines correspond to $E_Z = 0.1$ eV/Å. (*a*) — $T = 1000$ K. The lines *1, 2* and *3* correspond to the values τ_{adsorb} equal to, respectively $5 \cdot 10^{-8}$, $7 \cdot 10^{-8}$ and $8.661 \cdot 10^{-8}$ s. (*b*) — $T = 700$ K. The lines *1, 2* and *3* correspond to the values τ_{adsorb} equal, respectively, to $5 \cdot 10^{-6}$, $2 \cdot 10^{-5}$ and $3.563 \cdot 10^{-5}$ s. (*c*) — $T = 350$ K. The lines *1* and *2* correspond to the values τ_{adsorb} equal to 149 and 11400 s, respectively. The descending branch of the line *2* in the field Figure 2, *c* practically coincides with the vertical axis of the graph and is therefore invisible on the graph. The minimum of this line is reached at$Q = 0.023$, and the value $\Phi(Q = 0.023)/\Phi(Q = 0) = -74$.

Table 2. Characteristics of stationary points in equation (3)

	$T = 350$ K		$T = 700$ K		$T = 1000$ K	
E_Z, eV/Å	0	0.1	0	0.1	0	0.1
τ^c_{adsorb}, s	149	11400	$3.563 \cdot 10^{-5}$	$8.6 \cdot 10^{-6}$	$8.661 \cdot 10^{-8}$	$4.9 \cdot 10^{-8}$
Q^C	0.031	0.024	0.062	0.05	0.088	0.07

The decline of E_Z from 0.01 to 0.001 eV/Å is accompanied by a decrease in the interval of formation of an inhomogeneous distribution from 1350 c to 550 s. In this case, the saturation time of the sample with hydrogen varies slightly. Also, the concentration of hydrogen in EEF area practically does not change (this value is $Q \sim 0.03$).

5. Conclusion

The findings outlined in this paper indicate that exposure to an external electric field can effectively reduce the mutual attraction of atoms of adsorbed hydrogen. This decrease in the H-H interaction is able to suppress the process of saturation of graphene with hydrogen and create a deficiency of chemisorbed hydrogen in the irradiated areas. A necessary condition for achieving such a result is the effect of EEF throughout the entire hydrogenation process. Practically significant temperatures of the saturation process lie in the range of room temperatures. Calculations performed at constant values of temperature and desorption time show that at low amplitudes E_Z from 0.01 to 0.001 eV/Å it is practically impossible to achieve purity of the irradiated area better than 3 % of the residual hydrogen. Another serious limitation is the requirement of strict fulfillment of the condition (6). In this case, the term (6) of implementing the inhomogeneous distribution of hydrogen is only a necessary condition. Indeed, in the proposed regime, there are two stationary stable states in the irradiated region (the concentration of hydrogen in the first state is close to zero, and in the second to unity). Because of this ambiguity, the issue of stability of the boundary between the irradiated region with low hydrogen concentration and the non-irradiated region with high hydrogen concentration becomes disputable. Solving this issue is an individual problem and requires taking into account the surface diffusion of hydrogen atoms on the graphene surface through the interface of these regions. The effect of surface diffusion on the formation of an inhomogeneous distribution is expected to be reviewed in subsequent works.

Acknowledgments

The author expresses his thanks to K.P. Katin for discussion of the findings.

Funding

This study was performed as part of Priority 2030 program of National Research Nuclear University in MIFI.

Conflict of interest

The author declares that he has no conflict of interest.

References

[1] K.S. Novoselov, A.K. Geim, S.V. Morozov, D. Jiang, Y. Zhang, S.V. Dubonos, I.V. Grigorieva, A.A. Firsov. Science **306**, 666 (2004).
[2] A.E. Galashev, O.R. Rakhmanova. UFN, **184** 1045, (2014). (in Russian).
[3] K.S. Novoselov, A.K. Geim, S.V. Morozov, D. Jiang, M.I. Katsnelson, I.V. Grigorieva, S.V. Dubonos, A.A. Firsov. Nature **438**, 197 (2005).
[4] K.A. Krylova, L.R. Safina, R.T. Murzaev, S.A. Shcherbinin, J.A. Baimova, R.R. Mulyukov. Physics of the Solid State, **65** (9), 1514 (2023).
[5] K.G. Mikheev, R.G. Zonov, N.V. Chuchkalov, G.M. Mikheev. Phys. Solid State, **63**, 498 (2021). **66**, 280 (2024).
[6] S.Yu. Davydov. Physics of the Solid State, **66** (2), 293 (2024).
[7] S.Yu. Davydov, A.A. Lebedev. Physics of the Solid State, **65** (12), 1966 (2023).
[8] S.Yu. Davydov. Physics of the Solid State, **67** (2), 363 (2025).
[9] J.O. Sofo, A.S. Chaudhari, G.D. Barber. Phys. Rev. B**75**, 153401 (2007).
[10] D.C. Elias, R.R. Nair, T.M.G. Mohiuddin, S.V. Morozov, P. Blake, M.P. Halsall, A.C. Ferrari, D.W. Boukhvalov, M.I. Katsnelson, A.K. Geim, K.S. Novoselov. Science **323**, 610 (2009).
[11] D.W. Boukhvalov, M.I. Katsnelson, A.I. Lichtenstein. Phys. Rev. B**77**, 035427 (2008). DOI: https://doi.org/10.1103/PhysRevB.77.035427
[12] S. Casolo, O.M. Løvvik, R. Martinazzo, G.F. Tantardini. J. Chem. Phys. **130**, 054704 (2009). https://doi.org/10.1063/1.3072333
[13] L.A. Openov, A.I. Podlivaev. JETP Lett **90**, 459 (2009). DOI: 10.1134/S002136400918012X
[14] P. Chandrachud, B.S. Pujari, S. Haldar, B. Sanyal, D.G. Kanhere. J. Phys. Condens. Matter **22**, 465502 (2010). DOI 10.1088/0953-8984/22/46/465502
[15] A. Ranjbar, M.S. Bahramy, M. Khazaei, H. Mizuseki, Y. Kawazoe. Phys. Rev. B **82**, 165446 (2010). doi.org/10.1103/PhysRevB.82.165446
[16] Bo Liu, Julia A Baimova, S.V. Dmitriev, Xu Wang, Hongwei Zhu, Kun Zhou. J. Phys. D: Appl. Phys. **46**, 305302 (2013). doi:10.1088/0022-3727/46/30/305302
[17] S.Yu. Davydov. V.I. Margolin. Poverkhnost', **8**, 5 (1983). (in Russian).
[18] S.Yu. Davydov. FTT **59**, *4*, 825 (2017). (in Russian).
[19] S.Yu. Davydov. FTP **58**, *9*, 482 (2024). (in Russian).
[20] H. González-Herrero, E. Cortés-del Río, P. Mallet, J.-Y. Veuillen, P. Palacios, J. Gómez-Rodrıguez, I. Brihuega, F. Yndurain. 2D Materials **6**, *2*, 021004 (2019).
[21] L. Hornekær, E. Rauls, W. Xu, Ž. Šljivančanin, R. Otero, I. Stensgaard, E. Lægsgaard, B. Hammer, F. Besenbacher. Phys. Rev. Lett. **97**, 186102 (2006). DOI: 10.1103/PhysRevLett.97.186102
[22] Z.M. Ao, F.M. Peeters. Appl. Phys. Lett. **96**, 253106 (2010). doi: 10.1063/1.3456384
[23] A.I. Podlivaev, K.P. Katin. Appl. Surf. Sci. **686**, 162125 (2025). https://doi.org/10.1016/j.apsusc.2024.162125
[24] M.M. Maslov, A.I. Podlivaev, K.P. Katin. Molecular Simulation **42**, 305 (2016). DOI: 10.1080/08927022.2015.1044453
[25] A.I. Podlivaev, K.S. Grishakov, K.P. Katin, and M.M. Maslov. JETP Letters, **113** (3), 169 (2021). DOI: 10.1134/S0021364021030085

[26] K.P. Katin, K.S. Grishakov, A.I. Podlivaev, M.M. Maslov. J. Chem. Theory Comput. **16**, 2065 (2020). https://doi.org/10.1021/acs.jctc.9b01229
[27] A.I. Podlivaev & K.P. Katin. JETP Letters **92**, 52 (2010). DOI: 10.1134/S0021364010130102
[28] L.A. Openov, A.I. Podlivaev. Physics of the Solid State, **57** (7), 1477 (2015).
[29] A.I. Podlivaev and L.A. Openov. JETP Lett. **103**, 185 (2016).
[30] K.P. Katin, A.I. Kochaev, S. Kaya, K.I. Orlov, I.V. Bereznicczky, M.M. Maslov. Appl. Surf. Sci. **684**, 161923 (2025). DOI: 10.1016/j.apsusc.2024.161923
[31] E.M. Pearson, T. Halicioglu, W.A. Tiller. Phys. Rev. A**32**, 3030 (1985). DOI: https://doi.org/10.1103/PhysRevA.32.3030
[32] L.A. Openov, A.I. Podlivaev. Techn. Phys. Lett. **36**, 31 (2010).
[33] L.A. Bolshov, A.P. Napartovich, A.G. Naumovets, A.G. Fedorus. UFN. (in Russian). **122**, *1*, 125 (1977). https://www.mathnet.ru/ufn9670
[34] O.M. Braun, V.K. Medvedev. UFN, v. 157 (4), 631 (1989). (in Russian). https://www.mathnet.ru/ufn7641
[35] S.Yu. Davydov. Pisma v ZhTF **38**, *4*, 41 (2012). (in Russian).
[36] S.Yu. Davydov. Pisma v ZHTF, **40**, *13*, 52 (2014). (in Russian).

Translated by T.Zorina